Structure, Volume *27*

Supplemental Information

Structural Basis of CD160:HVEM Recognition

Weifeng Liu, Sarah C. Garrett, Elena V. Fedorov, Udupi A. Ramagopal, Scott J. Garforth, Jeffrey B. Bonanno, and Steven C. Almo

Supplemental information

Figure S1 related to Figure 2. Solution behavior and overall structure of CD160
(A) Different construct designs of human CD160. Top panel shows the scheme of the human CD160 ectodomain organization. Cross mark in the box (☒) before the construct design scheme indicates this construct was not successfully refolded, whereas checkmark in the box (☑) indicates successful refolding of the construct. (B) The purified S2 cell derived CD160 (I27-L158 with 6 × His tag) were subjected to reducing (R.) or non-reducing (N.R.) treatments and then SDS-PAGE analysis. (C) SEC-MALS analysis of the S2 cell derived CD160 demonstrates that the molecular weight of CD160 is 15.1 ± 0.9 KDa, corresponding to the calculated molecular weight of monomeric CD160. (D) The overall structures of two chains of CD160 in one asymmetry unit. (E) Superimposition of the structures of chain A and chain B of CD160 shows almost identical structures.

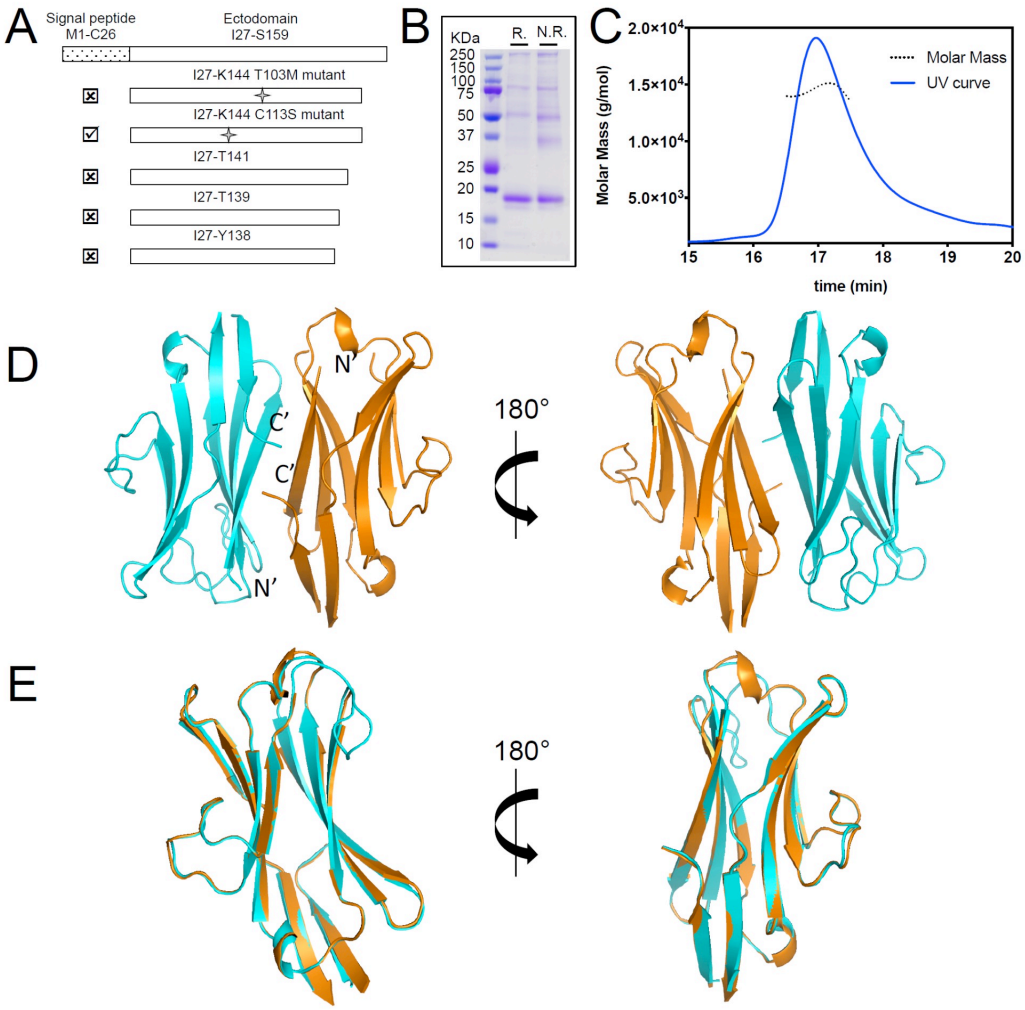

Figure S1.

Figure S2 related to Figure 3. Solution behavior of CD160 and comparison of CD160 and BTLA

(A) SPR results of injections of S2 derived CD160 (I27-L158 with 6 × His tag) across immobilized HVEM at various concentrations as indicated in the figure. (B) SEC traces of S2 derived CD160 (I27-L158 with 6 × His tag), HVEM and the mixtures of CD160 and HVEM in different molar ratios. (C) SEC traces of S2 derived CD160 (I27-L158 with 6 × His tag), LIGHT:HVEM mixture and the mixture of S2 derived CD160 (I27-L158 with 6 × His tag), LIGHT and HVEM. (D) SEC traces of refolded human BTLA, HVEM and the mixture of BTLA and HVEM. (E) Left panel: the structure of CD160 is presented as cartoon; the front sheet is colored as cyan and the back sheet is colored as orange; the connecting loops are colored as yellow. Middle panel: the structure of BTLA is presented as cartoon (PDB entry 2AW2); the front sheet is colored as red and the back sheet is colored as magenta; the connecting loops are colored as green. Right panel: superimposition of CD160 and BTLA.

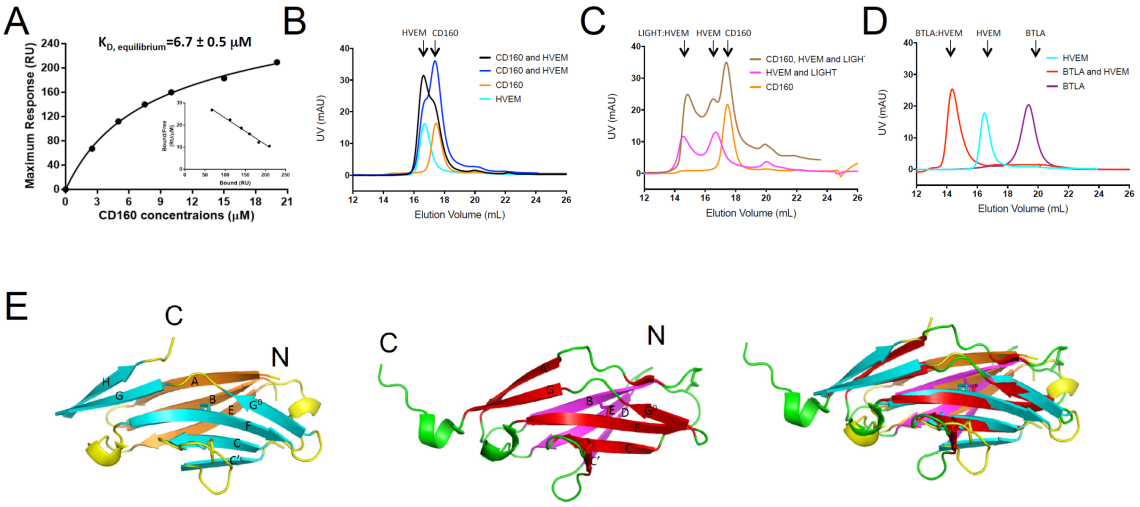

Figure S2.

Fig S3 related to Figure 4. Clear electron densities between the CD160:HVEM interface and superimposition of CD160:HVEM, BTLA:HVEM and HSV1-gD:HVEM complexes.

(A) HVEM is shown as blue cartoon and CD160 is shown as green cartoon. 2*Fo-Fc* electron density map was contoured at sigma 1.0 and shown as red mesh. (B) Superimposition of the HVEM structures from CD160:HVEM, BTLA:HVEM and gD:HVEM complexes. CD160 is shown as cyan and HVEM is shown as orange from CD160:HVEM structure. BTLA is shown as red and HVEM is shown as magenta from BTLA:HVEM structure. HSV1-gD is shown as yellow and HVEM is shown as grey from gD:HVEM structure.

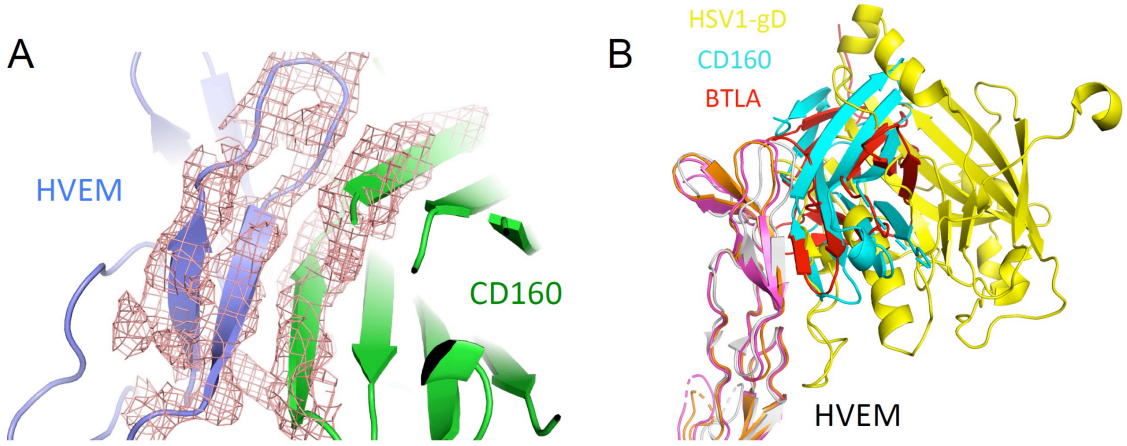

Fig S3.

Fig S4 related to Figure 5. Modeling of CD160/HVEM mutants and comparison of HVEM with other TNF receptors.

Modeling of CD160 Q124W mutant (A) and HVEM G72D mutant (B) shows steric conflicts of the side chains with other residues. The mutated residues are shown as lines and the potential steric collisions are indicated by red heptagons. (C) Protein sequence alignment of HVEM with other TNF receptors. (D) Structural superimposition of human HVEM from CD160:HVEM complex (orange) with ELR1 (magenta; PDB entry 3WVT and chain A), human CD40 (yellow; PDB entry 6FAX and chain R), human TNFR2 (green; PDB entry 3ALQ and chain R) and human LTβR (salmon; PDB entry 4MXW and chain S). Residues G72-P77 of HVEM are shown as sticks. (E) Zoom in view of the superimposition, which emphasizes the HVEM G72 residue. (F) Zoom in view of the HVEM G72 homologous showing the potential steric effect posed by other TNF receptor G72 homologous residues.

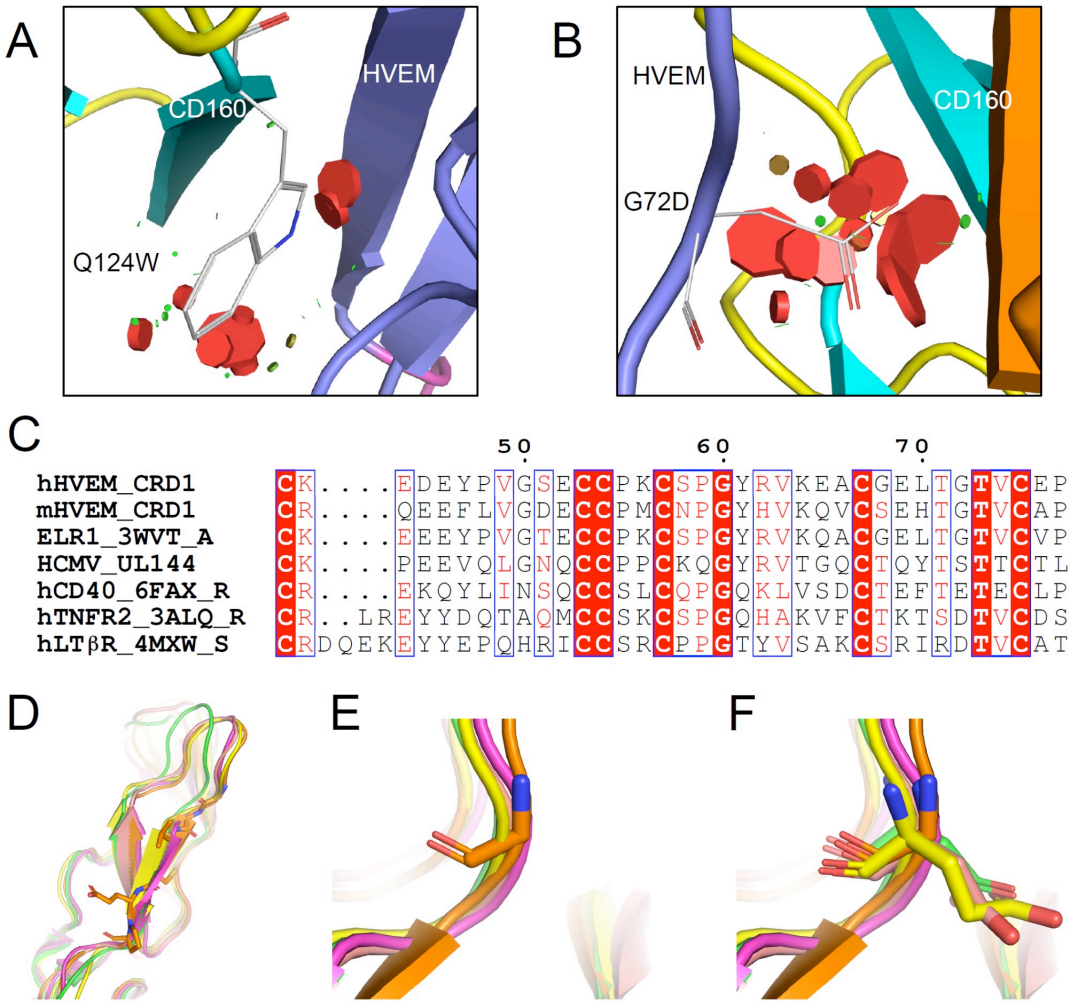

Fig S4.